Dual-thread parallel control strategy for ophthalmic adaptive optics

Yongxin Yu (于永新)[1,2*] and Yuhua Zhang (张宇华)[2]

[1]*School of Computer Science and Technology, Tianjin University, Tianjin 300072, China*
[2]*Department of Ophthalmology, University of Alabama at Birmingham, Birmingham, AL 35294, USA*
Corresponding author: yyx@tju.edu.cn

Received July 19, 2014; accepted October 11, 2014; posted online November 28, 2014

To improve ophthalmic adaptive optics (AO) speed and compensate for ocular wavefront aberration of high temporal frequency, the AO wavefront correction is implemented with a control scheme including two parallel threads: one is dedicated to wavefront detection and the other conducts wavefront reconstruction and compensation. With a custom Shack–Hartmann wavefront sensor that measures the ocular wave aberration with 193 subapertures across the pupil, AO achieves a closed-loop updating frequency up to 110 Hz, and demonstrates robust compensation for ocular wave aberration up to 50 Hz in an AO scanning laser ophthalmoscope.

OCIS codes: 120.3890, 170.0110, 220.1000, 220.1080.
doi: 10.3788/COL201412.121202.

Adaptive optics (AO) was originally conceived for improving the spatial resolution of astronomy imaging by compensation for the time-varying wavefront aberration induced by the atmosphere turbulence[1]. It has been applied to correct the wavefront aberration of the living human eye's optics[2] and enabled diffraction-limited imaging in a variety of retina imaging modalities, including AO flood illumination funds camera[2–4], AO scanning laser ophthalmoscope (AOSLO)[5–7], and AO optical coherence tomography[8–11]. A major advantage of AO assisted ophthalmoscopy is that AO can compensate for the individual eye's optical defects that vary from person to person thereby allowing for personalized optimal imaging quality. AO worked with a quasi-static mode in early AO retinal imaging systems in which AO was operated to minimize the static ocular wavefront aberration through several (tens of) loops of iteration and stopped to let the frame grabber to acquire the images[2,5]. In fact, the living human eye's wavefront aberrations are not static but dynamic. Hofer *et al.* assessed the wavefront dynamics using a Shack–Hartmann wavefront sensor with a frame rate of 25.6 Hz[12]. They found that the highest frequency of the ocular wavefront aberration was approximately 5–6 Hz. Thus, they suggested that an AO system with a closed-loop bandwidth of 1–2 Hz could correct the aberrations to achieve diffraction-limited imaging. However, Diaz-Santana *et al.* later found that the frequency of the ocular wavefront aberration could be as high as to 30 Hz by measuring the ocular wavefront using a high-speed Shack–Hartmann wavefront sensor[13]. Their finding was reverberated by the study conducted by Nirmaier *et al.*[14] These results indicate that high-speed AO correction speed is required for better compensation for high-frequency wavefront aberrations thereby further improving the imaging quality.

Advanced control strategy can play a critical role in high-speed AO system. In general, an AO system consists of a wavefront sensor that measures the wavefront shape of the imaging light and a wavefront compensator that "nulls" the aberration[15]. The (residual) aberration is measured continuously by the wavefront sensor and fed to the wavefront compensator, forming a feedback closed loop. For ophthalmic imaging, a classic wavefront detector is a Shack–Hartmann wavefront sensor and the wavefront compensator is typically a deformable mirror (DM). As a dynamic control system, the temporal bandwidth of the AO closed loop, a measure of how rapidly the correction must be updated, should be sufficiently wide so that the time-varying wavefront aberrations can be corrected. Normally, the −3 dB bandwidth of AO system should be 3–10 times of the highest frequency of the ocular wavefront aberration[16]. A classic AO loop includes three steps that are carried out sequentially, namely, wavefront detection, reconstruction, and compensation[15]. Thus, the AO bandwidth is determined by the time consumed at each step. With the advancement of high-speed DM manufacture technology, for example, the micro-electric–mechanic system-based DM (Multi-DM series, Boston Micromachines Co., Cambridge, MA, USA) or the electric–magnetic DM (Alpao Hi-speed DM series, Alpao SAS, France), the setting time can be less than 1 ms within +/5%, implying that the time for single-step wavefront compensation (i.e., the DM actuation) is negligible. Thus, AO close-loop frequency f_l in the sequential operation may be estimated by $1/(t_d + t_r)$, where t_d is the wavefront detection time and t_r is the wavefront reconstruction time. In general, t_d is determined by the light power for wavefront sensing that is ultimately decided by the eye safety limit, the sensitivity of the wavefront sensor camera, and the overall

light budget depending on the specific imaging system. t_r is dominated by the number of subaperture or sampling points over the pupil, the number of pixels within individual subaperture, and the overall number of pixels within the pupil, as well as the number of the actuators of the DM. In most AO retinal imaging systems, the closed-loop updating frequency is less than 30 Hz[3,4,6,7,9,17]. To accelerate the AO speed, we present a parallel control structure consisting of two independent threads: one contains the wavefront detection (camera exposure) and the other contains wavefront reconstruction (deriving the DM actuator commands from the measured wavefront) and compensation (DM actuation). The wavefront sensor is operated with a continuous and independent (from the wavefront reconstruction and compensation) exposure mode, and the wavefront reconstruction and the DM actuation are informed by the end of each exposure period.

The experiment was conducted with an AOSLO system that has been reported elsewhere[10] (Fig. 1). The light source for retinal imaging and wavefront sensing was a superluminescent diode (SLD) (Broadlighter S840-HP, Superlum Ltd, Russia). Its center wavelength is at 840 nm and the bandwidth is of 50 nm. The light is delivered to the eye through the scanning optics and the DM and forms a scanning raster on the retina. The diffusely reflected light from the retina transmitts inversely along the ingoing path to the beam splitter, where most of the light passed through and is relayed to the collection lens. A confocal pinhole is placed at the focal point of the collection lens, and the signal is received by a photomultiplier tube (PMT) (H7422-50, Hamamatsu, Japan), further processed, and acquired by the computer. The pupil size of the instrument is 6 mm in diameter. The AO comprises of a DM (Hi-Speed DM97-15, ALPAO SAS, France) and a custom Shack–Hartmann wavefront sensor. The wavefront sensor was made up of a high-speed CMOS camera (MicroVista®-NIR, Intevac Inc., USA) whose spectral response is optimized for the near-infrared imaging light. A lenslet array of 0.3×0.3 (mm) patch and 7.6 mm focal length samples the wavefront in 193 subapertures with a 512×512 pixel sensor. The influence function was obtained by measuring the wavefront response on the wavefront sensor induced by each individual actuators[18]. With a nearly flat wavefront of a model eye made up with a lens and a diffuse scatterer placed at the focal plane, each actuator was pushed and pulled, and the corresponding deflection of the light spots on the Shack-Hartmann wavefront sensor was recorded. Listing the deflections of all subapertures over the pupil that were generated by an individual actuator in a column, and putting all the columns that were generate by all actuators together, we thus formed the system influence or interaction matrix. Since there were 193 subapertures and 97 actuators, each subaperture estimated both x and y deflections, the dimensions of influence matrix were 386×97. Wavefront reconstruction strategy presented by Li *et al.*[18] was adopted to derive the command for actuating the DM.

The CMOS camera of the Shack–Hartmann wavefront sensor operates with a rolling shutter mode in which the image data are read out sequentially row by row. All rows of the CMOS sensor have the same amount of exposure time. Once the data in a row are read out, the camera resets this row and starts to integrate light with the set exposure time. Then the row is accessed again in the next image frame. With a 512×512 pixels configuration, the total time for reading data is 7.7 ms, thus the highest frame rate is 129 frames per second. In our application, we operated the camera with an emulated snapshot shutter (or globe shutter) mode. In this mode, if we set an exposure time E ms, all rows will be exposing for (the same) time from time $t = 7.7$ ms to E. Thus, to ensure a simultaneous exposure, the exposure time should be greater than 7.7 ms. In our system, the minimum exposure time is 8.8 ms, which allows for 1.1 ms simultaneous exposure to all rows of the sensor.

Figure 2 shows the dual-threads control structure. One thread is for wavefront detection and the other for wavefront reconstruction and compensation. These two threads communicate by user-defined windows message. The wavefront detection includes three steps: light integration, data reading, and camera reset. The wavefront reconstruction involves background subtraction, calculation of the centroids' positions of the light spots of each subaperture, and calculation of the actuator commands. The wavefront compensation is carried out by the actuation of the DM. The wavefront sensor camera is set with a continuous exposure mode, serving as the

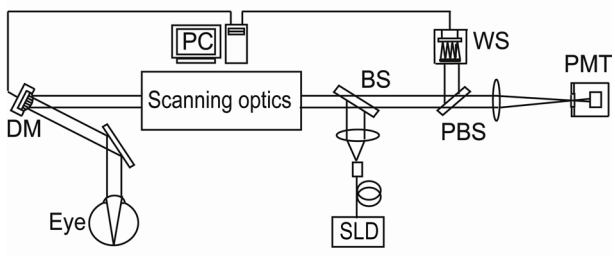

Fig. 1. AOSLO system diagram. PC, personal computer; BS, beam splitter; PBS, pellicle beam splitter; WS, wavefront sensor.

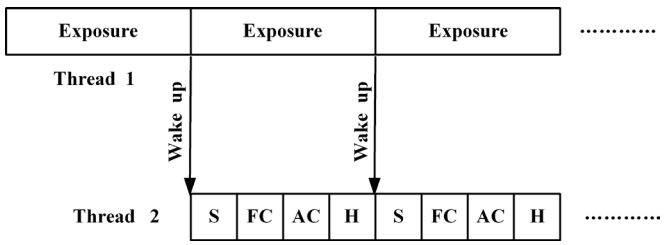

Fig. 2. Dual-threads AO control. S, substrate background; FC, find centroid; H, hang up; AC, calculate actuator command and actuate DM.

Table 1. AO Closed-loop Frequency

Exposure Time (ms)	AO Loop Frequency (Hz)
8.8	112.71
10	99.19
15	66.17
20	49.60
25	39.73

master loop (clock) in the two threads. The wavefront reconstruction and compensation thread starts first and turns to hang-up status and waits for wake-up message. Then the wavefront detection thread starts, after integration of the light, it sends a message to trigger wavefront reconstruction and compensation thread. Once the DM is actuated with the commands derived from the wavefront reconstruction, this thread hangs up and waits for next wake-up signal. The system works essentially with a 1-step delay scheme. The total time for wavefront construction and compensation is approximately 6.5 ms: the subtraction of background takes 1.5 ms and the calculation of centroids' positions takes 4.5 ms, the computation of the actuation commends and the actuation of the DM take less than 0.5 ms. Thus, with a sequential control, the highest update frequency of the AO closed loop can be 65 Hz only. With the parallel dual-thread algorithm, the AO closed loop can be operated at a frequency up to 110 Hz. Table 1 shows the updating frequency tested with the AOSLO in the living human eye.

The imaging light power measured at the cornea is 500 μW, which is about 1/26 of the maximum permitted exposure limits set by the ANSI standard. The AOSLO records continuous videos from the eye with a frame rate of 15 Hz. An uncoated pellicle beam splitter is used to pick up 8% of the light reflected from the human eye for wavefront measurement. With a closed-loop updating frequency of 110 Hz, AO can reduce the root-mean-square (RMS) wave aberration to less than 50 nm in most eyes, meeting the Maréchal criterion[19], which indicates that when the RMS wave aberration is less than 1/14 wavelength the imaging is diffraction limited (Fig. 3).

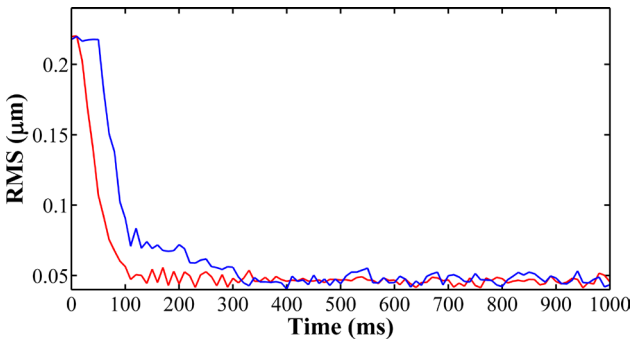

Fig. 3. RMS traces of AO closed loop of 100 (red line) and 20 Hz (blue line) tested with a model eye. When AO is operated at 100 Hz, it reduces the RMS of the wavefront aberration to less than 0.05 μm within 100 ms.

We imaged five human subjects with healthy eyes using the AOSLO with the new control algorithm. The study followed the tenets of the Declaration of Helsinki and was approved by the Institutional Review Board at the University of Alabama at Birmingham. Written informed consent was obtained from participants after the nature and possible consequences of the study were explained. Retinal images were acquired under dilatation (one topically applied drop each of 1% tropicamide and 2.5% phenylephrine). Exemplary images of AO correction at 100 Hz are shown in Fig. 4. The robust

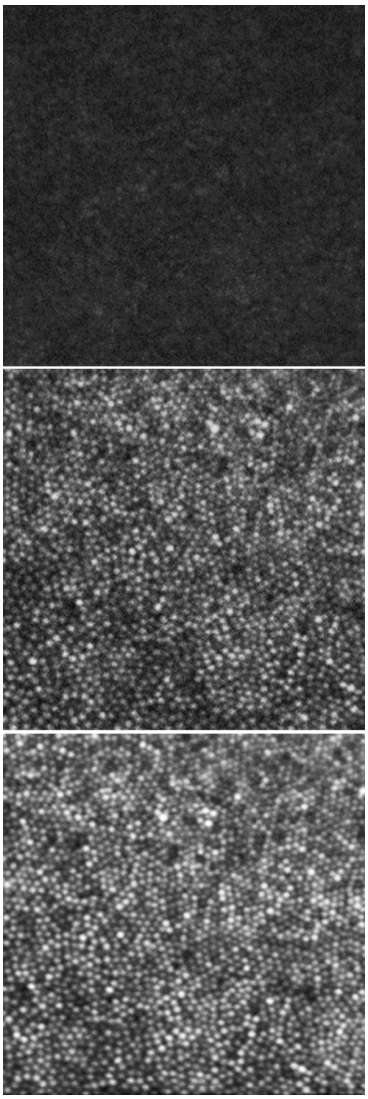

Fig. 4. Retinal images taken with the AOSLO. The top panel is a single frame taken before AO correction, middle panel is a single frame taken after AO correction, and the bottom panel is a registered set of 20 AO-corrected images. All images have been corrected for distortions due to eye movements[20]. These images were taken from a retinal location about 0.5° nasally away from the fovea center. The field of view subtends 0.7°, or approximately 210 μm on a side.

performance of the new AO control algorithm was evidenced by the significantly improved resolution, brightness, and contrast. Wavefront aberrations before and after AO correction were recoded. The corresponding components of the Fourier transform of the wavefront aberrations after and before AO correction were compared and expressed as the power rejection ratio, that is, $\omega_a(f)/\omega_b(f)$, where $\omega_a(f)$ and $\omega_b(f)$ are the Fourier transform components of the RMS wavefront aberrations after and before AO correction (Fig. 5), respectively. Evidently, the power rejection ratios of the Fourier components of the aberrations within 0–50 Hz are less than 1, indicating that all frequency components were compressed by the AO compensation.

We have demonstrated a parallel control strategy that enables high-speed AO correction. This may be an important step for further improving AO retinal imaging quality. While low-speed AO systems have demonstrated decent correction previously due to the power spectrum of the ocular wavefront aberration concentrating in the low frequency region, retinal imaging may still be further benefited from high-speed AO. If the temporal frequency of the ocular aberration is up to 30 Hz, the AO closed-loop updating rate should be at least 90 Hz. To correct for the wavefront aberration precisely, the wavefront should be measured with adequate spatial samplings. Thus, an ideal wavefront sensor should possess fast frame rate and high-density spatial subapertures. We should note that a high frame rate of the wavefront sensor camera is important but it is not the sole factor for achieving robust AO correction. Diaz-Santana *et al.* reported a 240 Hz frame rate of their wavefront sensor, but they achieved it on a 128×128 pixels sensor with only 21 subapertures over the pupil[13], which is inadequate for compensating for aberrations of high spatial frequency or high order. In our study, we measured the wavefront with 193 subapertures over the pupil using a sensor with 512×512 pixels and high frame rates, meeting the spatial and temporal requirements of an AO system.

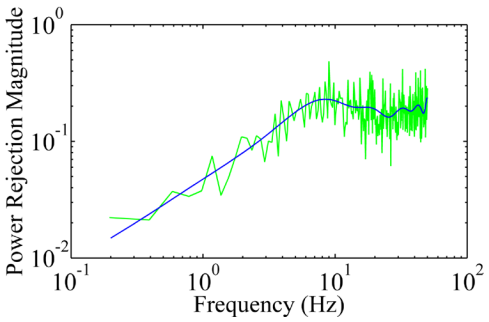

Fig. 5. Power rejection ratio of ocular wavefront aberration with AO operating at 100 Hz. The green line is the mean ratios of individual frequency components obtained from the five eyes of the study subjects. The blue curve is a fitting of 15 orders of power series.

While we demonstrated the technical advance, we also noted the limitations of our study. Firstly, due to the rolling shutter exposure and data reading mechanism of the CMOS camera, the wavefront detection may be susceptible to certain motion artifacts in measurement of fast wavefront aberrations. Secondly, because the camera is running with a continuous exposure mode, the actuation of DM happens during the exposure of the camera, thus the accuracy of wavefront measurement may be affected. Ideally, the camera should receive a message from the wavefront reconstruction and compensation thread to quickly stop and resume light integration, but this camera unfortunately does not possess this capability that allows us to do so. Despite these drawbacks, the retinal image quality is comparable to that acquired with strict sequential AO correction. With new cameras of faster frame rate, higher sensitivity, and more flexible control functions, we may further enhance AO performance and thereby improving retinal image quality.

As a pilot study for improving AO performance, we were unable to provide a quantitative estimation of the benefit of the fast AO bringing in for the retinal image quality. It should be noted that high-speed AO correction is a necessary but not a sufficient condition for high-quality retinal imaging through the living human eye. In addition to the ocular wavefront aberration, other factors such as the clarity of the lens and the vitreous, the uniformity of the team film, and the eye motion can also impose significant impact on the image quality. For example, even in an emmetropic eye of a young subject, the imaging brightness can be significantly varying within a very short time period due to tear film changing. Under this situation, it is difficult to objectively estimate the improvement brought in by the fast AO through a simple comparison of the retinal images obtained with the fast correction and a slower correction. Thus, we must acknowledge the fact that the benefit of the fast AO is yet to be proven. Nevertheless, high speed is indeed important for high-quality imaging theoretically and practically. As proven by previous studies, the high-frequency dynamics of the ocular wavefront aberration demands fast AO. High-speed updating frequency can facilitate and enhance advanced control algorithm and strategy[21,22]. Fast AO may be applied to new imaging system, which is very promising to achieve high-speed retinal imaging[23].

In conclusion, we develop a parallel control algorithm for increasing the AO closed-loop speed and demonstrate its robust performance for correcting the ocular wavefront in the living human eye. This method may allow us to take full advantage of the speed of the camera, thereby allowing for AO correction for ocular aberration of high temporal frequency.

This work was supported by funding from the Eye-Sight Foundation of Alabama (YZ), the International Retina Research Foundation (YZ), NIH 5R21EY021903

(YZ), and institutional support from the Research to Prevent Blindness, the EyeSight Foundation of Alabama, the Buck Trust of Alabama, and NIH P30 EY003039. Yongxin Yu was supported by a visiting scholarship fund from Tianjin University and the University of Alabama at Birmingham Exchange Scholar Program.

References

1. H. W. Babcock, Publ. Astron. Soc. Pac. **65,** 229 (1953).
2. J. Liang, D. R. Williams, and D. T. Miller, J. Opt. Soc. Am. A Opt. Image Sci. Vis. **14,** 2884 (1997).
3. H. Hofer, L. Chen, G. Y. Yoon, B. Singer, Y. Yamauchi, and D. R. Williams, Opt. Express **8,** 631 (2001).
4. J. Rha, R. S. Jonnal, K. E. Thorn, J. Qu, Y. Zhang, and D. T. Miller, Opt. Express **14,** 4552 (2006).
5. A. Roorda, F. R. Borja, W. D. Iii, H. Queener, T. Hebert, and M. Campbell, Opt. Express **10,** 405 (2002).
6. Y. Zhang, S. Poonja, and A. Roorda, Opt. Lett. **31,** 1268 (2006).
7. S. A. Burns, R. Tumbar, A. E. Elsner, D. Ferguson, and D. X. Hammer, J. Opt. Soc. Am. A Opt. Image Sci. Vision **24,** 1313 (2007).
8. B. Hermann, E. J. Fernández, A. Unterhuber, H. Sattmann, A. F. Fercher, W. Drexler, P. M. Prieto, and P. Artal, Opt. Lett. **29,** 2142 (2004).
9. D. T. Miller, O. P. Kocaoglu, Q. Wang, and S. Lee, Eye **25,** 321 (2011).
10. A. Meadway, C. A. Girkin, and Y. Zhang, Opt. Express **21,** 29792 (2013).
11. G. Shi, Y. Dai, L. Wang, Z. Ding, X. Rao, and Y. Zhang, Chin. Opt. Lett. **6,** 424 (2008).
12. H. Hofer, P. Artal, B. Singer, J. L. Aragón, and D. R. Williams, J. Opt. Soc. Am. A Opt. Image Sci. Vis. **18,** 497 (2001).
13. L. Diaz-Santana, C. Torti, I. Munro, P. Gasson, and C. Dainty, Opt. Express **11,** 2597 (2003).
14. T. Nirmaier, G. Pudasaini, and J. Bille, Opt. Express **11,** 2704 (2003).
15. R. K. Tyson, *Principles of Adaptive Optics* (CRC Press, 2011).
16. F. Golnaraghi and B. C. Kuo, *Automatic Control Systems* (Wiley, 2009).
17. A. Dubra and Y. Sulai, Biomed. Opt. Express **2,** 1757 (2011).
18. K. Y. Li, S. Mishra, P. Tiruveedhula, and A. Roorda, in *Proceedings of American Control Conference* 3848 (2009).
19. R. R. Shannon and J. C. Wyant, *Applied Optics and Optical Engineering* (Academic Press, 1980).
20. C. R. Vogel, D. W. Arathorn, A. Roorda, and A. Parker, Opt. Express **14,** 487 (2006).
21. W. Zou and S. A. Burns, Opt. Express **17,** 20167 (2009).
22. Z. Zheng, C. Li, B. Li, and S. Zhang, Chin. Opt. Lett. **11,** 110101 (2013).
23. Y. He, H. Li, J. Lu, G. Shi, and Y. Zhang, Chin. Opt. Lett. **11,** 021101 (2013).